Fully Transparent Quantum Dot Light-Emitting Diode Integrated with Graphene Anode and Cathode

Jung-Tak Seo,[†] Junebeom Han,[§] Taekyung Lim,[§] Ki-Heon Lee,[‡] Jungseek Hwang,[†] Heesun Yang,[‡] and Sanghyun Ju*[,§]

[†]Department of Physics, Sungkyunkwan University, Suwon, Gyeonggi-Do 440-746, Republic of Korea, [‡]Department of Materials Science and Engineering, Hongik University, Seoul 121-791, Republic of Korea, and [§]Department of Physics, Kyonggi University, Suwon, Gyeonggi-Do 443-760, Republic of Korea

ABSTRACT A fully transparent quantum dot light-emitting diode (QD-LED) was fabricated by incorporating two types (anode and cathode) of graphene-based electrodes, which were controlled in their work functions and sheet resistances. Either gold nanoparticles or silver nanowires were inserted between layers of graphene to control the work function, whereas the sheet resistance was determined by the number of graphene layers. The inserted gold nanoparticles or silver nanowires in graphene films caused a charge transfer and changed the work function to 4.9 and 4.3 eV, respectively, from the original work function (4.5 eV) of pristine graphene. Moreover the sheet resistance values for the anode and cathode electrodes were improved from ~63 000 to ~110 Ω/sq and from ~100 000 to ~741 Ω/sq as the number of graphene layers increased from 1 to 12 and from 1 to 8, respectively. The main peak wavelength, luminance, current efficiency, and optical transmittance of the fully transparent QD-LED integrated with graphene anode and cathode were 535 nm, ~358 cd/m^2, ~0.45 cd/A, and 70−80%, respectively. The findings of the study are expected to lay a foundation for the production of high-efficiency, fully transparent, and flexible displays using graphene-based electrodes.

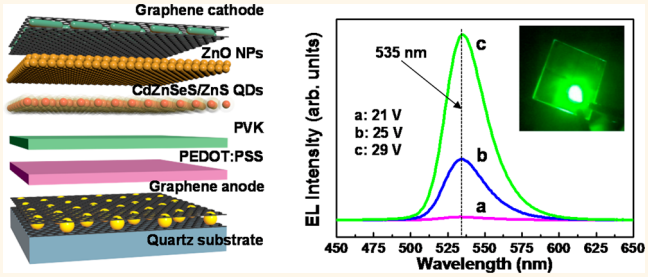

KEYWORDS: graphene · transparent electrode · work function · quantum dot · light-emitting device

In recent years, substantial progress has been made toward electrically driven quantum dot light-emitting diodes (QD-LEDs), which are regarded as a next-generation display technology, primarily because they can provide exceptional color reproducibility compared with state-of-the art organic LED (OLED) devices.[1,2] In order to fabricate flexible and transparent OLEDs and QD-LEDs, the development of new transparent electrodes using carbon nanotubes,[3,4] metal (e.g., copper[5] or silver[6]) nanowire networks, metal−semiconductor hybrids (Ag-NW/ZnO[7]), and graphene[8,9] has been actively persued. Specifically, many studies have recently been carried out to develop transparent electrodes using the advantageous features of graphene (sp^2-hybridized carbon atoms arranged in two dimension), such as high mobility, mechanical flexibility, and optical transparency.[9,10] With constantly increasing demand for transparent-electrode materials, it has been well established that graphene is, in particular, the most promising substitute for indium tin oxide (ITO), a depleting resource. Moreover, graphene has great potential as a flexible device material, owing to its excellent mechanical characteristics including flexibility and stretchability, as well as its high current capacity, none of which are exhibited in ITO. Graphene may also exhibit high transmittance and low sheet resistance and, importantly, an easily controllable work function, so that a high or low work-function material could be achieved for anode or cathode electrodes, respectively, for LEDs or solar cells.[11] Thus, by using properly work-function-controlled graphene sheets as anodes and cathodes, the injection barrier of holes or electrons may be reduced to enhance the device efficiency of LEDs.

Because a range of methods for controlling the work function and sheet resistance of graphene has lately been developed,[11−14]

* Address correspondence to shju@kgu.ac.kr.

Received for review September 19, 2014 and accepted November 26, 2014.

Published online November 26, 2014
10.1021/nn505316q

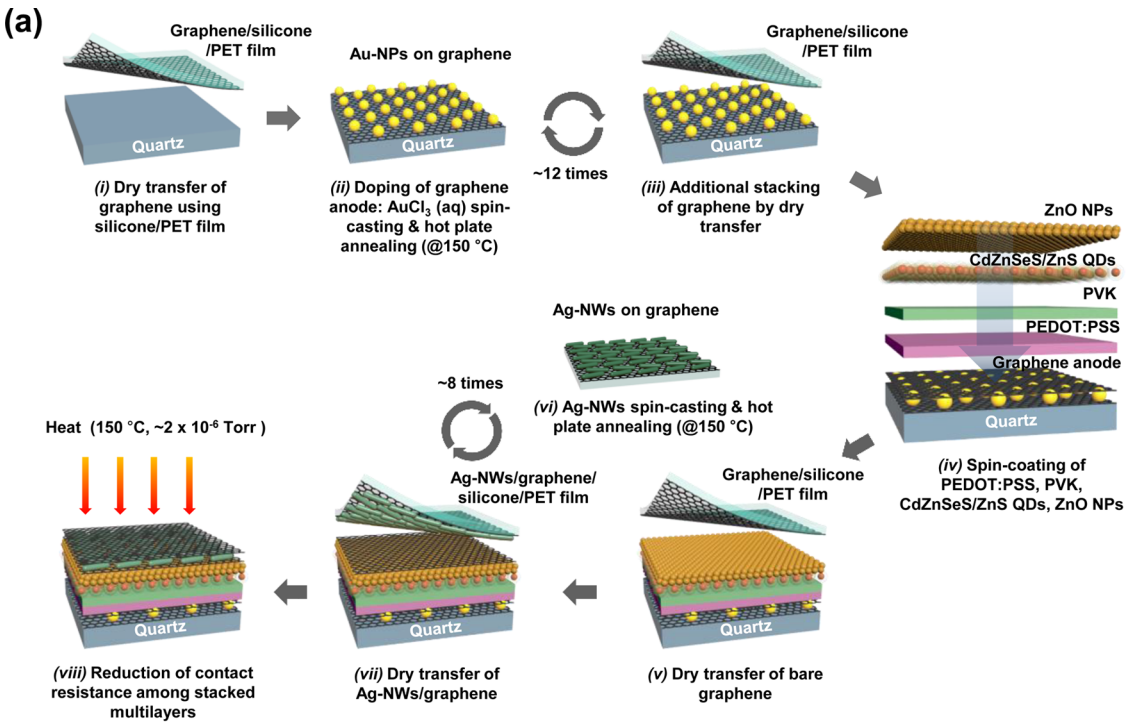

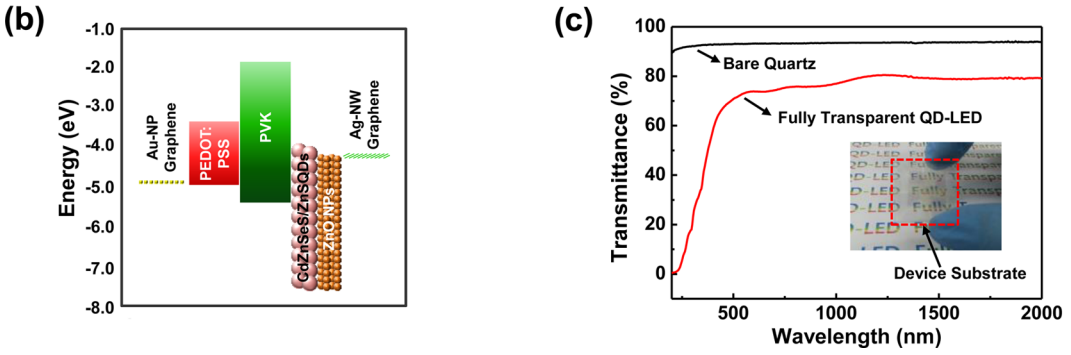

Figure 1. (a) Overall fabrication process for a QD-LED with graphene electrodes. (b) Energy levels of a multilayer-structured QD-LED. The HOMO and LUMO levels of PEDOT/PSS, PVK, CdZnSeS/ZnS QDs, and ZnO NPs are taken from ref 29. (c) Transmittance spectra of our QD-LED and quartz substrate. The inset shows a photograph of our QD-LED.

several LED devices using graphene as a transparent electrode have been fabricated.[15−19] However, these studies were limited in that graphene was only applied to nontransparent LEDs: graphene was only used as a transparent anode, whereas opaque metals such as LiF/aluminum were used as cathodes. In this regard, the development of LEDs using graphene as both anode and cathode should help realize fully transparent display devices.

In this study, we report an unprecedented fabrication of a fully transparent QD-LED with the use of work-function/sheet-resistance-controlled graphene films for both the anode and cathode. Among various methods for transferring graphene,[20,21] we adopted a dry-transfer process using silicone/polyethylene terephthalate (PET) film, which relies solely on the van der Waals force exerted by the silicone surface of a silicone/PET film. Methods for controlling the work function and sheet resistance of graphene, doping with gold nanoparticles and silver nanowires and varying the number of graphene layers, respectively, were introduced. Finally, the optical and electrical characteristics of the fabricated anode and cathode electrodes were examined, along with the display characteristics of the fully transparent QD-LED, such as electroluminescence, luminance, current efficiency, and the Commission Internationale de l'Eclairage (CIE) color coordinates.

RESULTS AND DISCUSSION

Figure 1a shows the fabrication process of the fully transparent QD-LED device, including a graphene anode and cathode. The process is as follows: (i) formation of the graphene anode by the dry-transfer method; (ii) fabrication of active layers of QD-LED using the spin-coating method; (iii) formation of the graphene cathode by the dry-transfer method and dry

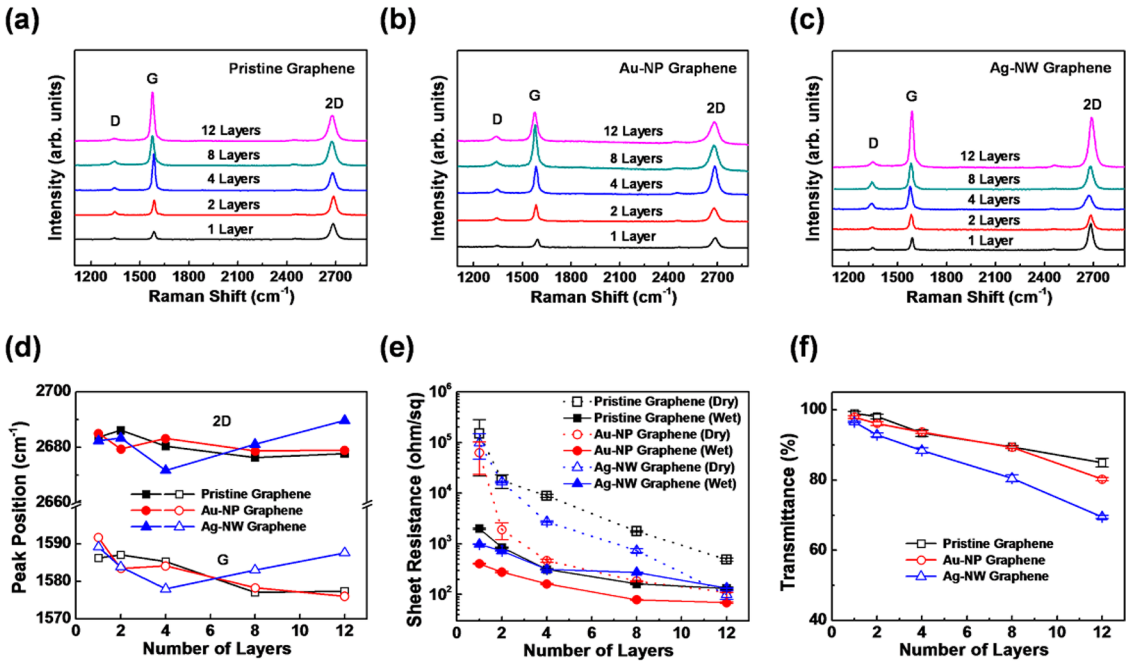

Figure 2. Raman spectra of (a) pristine graphene, (b) graphene doped with Au-NPs, and (c) graphene doped with Ag-NWs with 1, 2, 4, 8, and 12 layers. (d) Positions of the G and 2D peaks of pristine graphene, Au-NP graphene, and Ag-NW graphene as a function of the number of layers. (e) Sheet resistances of pristine, Au-NP, and Ag-NW graphene films prepared by the wet and dry fabrication methods as a function of the number of layers. (f) Transmittance data at 535 nm as a function of the number of layers for the three types of samples.

etching, through which the emissive areas are defined as the overlapped areas between the cathode and anode. Figure 1b shows the energy levels of the individual layers comprising the resultant QD-LED. The injection barrier between the graphene anode (~12 layers), with layer-by-layer Au-NP doping, and PEDOT/PSS used as a hole injection layer, was no more than 0.1 eV, whereas the barrier between the Ag-NW doped graphene cathode (~8 layers) and the ZnO nanoparticles used as an electron transfer layer was ~0 eV. This indicates that the injection of holes and electrons from anode and cathode to the hole-injection layer and electron-transport layer can be performed very efficiently. Consequently, graphene electrodes that have a suitable work-function difference between the anode and cathode were successfully fabricated using dopants with opposite charge transfer directions. In Figure 1c, the optical transmittance characteristics of bare quartz and fabricated display devices are compared. While the bare quartz exhibits a consistent transmittance of 93% within the scanned spectral range of 200−2000 nm wavelength, the display device shows two different aspects: decreasing transmittance in the range of 200−500 nm due to the combination of exciton in graphene and absorptions by active layers, and a constant transmittance of 70−80% in the 500−2000 nm range. Still, as seen in the inset of Figure 1c, the backside image of the fabricated device appears very clear without optical loss in the visible-light range.

Figure 2 shows changes in Raman, electrical, and optical characteristics caused by doping of anode and cathode graphene used in the fabrication of the transparent QD-LED device and by varying the number of graphene layers. Figure 2a−c shows Raman spectroscopy results for both graphene samples made by layer-by-layer doping with Au-NP and Ag-NW and pristine graphene layers as a comparison group (all with an equal number of layers). To verify the effects of varying the numbers of layers on the Raman spectra, Raman measurements for each sample set (pristine, Au-NP, and Ag-NW graphene) were conducted for the number of graphene layers 1, 2, 4, 8, and 12. As a result, it was verified that the shape of the 2D peak showed almost no change with increasing the number of graphene layers, regardless of sample type. This indicates that the hexagonal lattice of each layer was randomly oriented. Also we can observe that the increased number of graphene layers led to an overall increase of the intensity ratio $I(G)/I(2D)$, which can be explained by the intensity increment of the G mode of graphene with increasing number of layers.[22]

Meanwhile, Figure 2d shows the G and 2D peak positions of pristine, Au-NP, and Ag-NW graphene samples as a function of layers. In cases with less than four graphene layers, added layers caused a red-shift of the G and 2D peak positions. It is assumed here that a chemical-vapor-deposited graphene, when it is transferred and annealed at 150 °C on a SiO_2 substrate, is naturally hole-doped.[23−25] Figure 3 also reiterates the overall decreasing trend of the work function of 8- and 12-layer graphene without doping; the secondary electron cutoff is shifted slightly to a higher binding

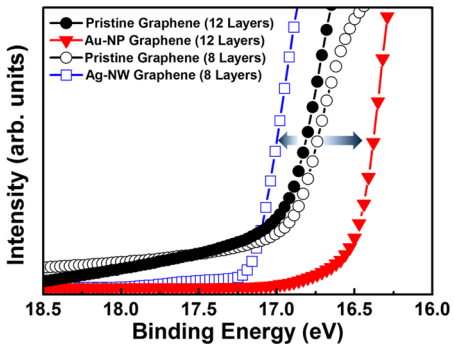

Figure 3. UPS spectra around the secondary-electron threshold region for two pristine graphene films with 8 and 12 layers, Ag-NW graphene film for cathode (8 layers), and Au-NP graphene film for anode (12 layers).

energy. This phenomenon can be observed when the hole concentration of graphene declines and consequently the Fermi level approaches the Dirac point.[23] In this regard, the red shift can be explained as follows: as the number of graphene layers increases, the underlying graphene layers screen the hole doping tendency from the SiO_2 substrate, and the proportion of charge-neutral graphene layers becomes larger for being stationed far from the substrate. Thus, it can be inferred that the decrease of hole concentration within graphene caused the red shifts of the G and 2D peaks.[23] While the pristine and Au-NP graphene exhibit a gradual red shift as the layer number increases, Ag-NW graphene shows blue shifts of G and 2D peaks for more than four layers, which can be caused by change in charge carrier type in graphene. When Ag-NWs with relatively low work function (or relatively high Fermi level) compared with pristine graphene contacted with graphene, negative charge transfer toward graphene occurs. This charge transfer decreases hole concentration and increases electron concentration in the graphene. Consequently, the Fermi level of the graphene, which was located below the charge neutral point (i.e., the Dirac point) until four layers, moves above the point when the number of layers is greater than four.[23] The opposite charge transfer directions caused by Au-NPs and Ag-NWs are confirmed by our ultraviolet photoelectron spectroscopy (UPS) measurements displayed in Figure 3.

Figure 2e shows the variations of sheet resistances of pristine, Au-NP doped, and Ag-NW doped graphenes formed by two different methods with varying layer as a function of the number of layers (dry-transfer method involving silicone/PET films used in this study and a previously tested wet-transfer method using PMMA and acetone for the transfer of CVD graphene, refer to the Experimental Section). The sheet resistance values of single-layered pristine graphene, a Ag-NW graphene, and a Au-NP graphene prepared by the dry transfer process were ~150 000, ~98 000, and ~63 000 Ω/sq respectively, and those by the wet process were ~2000, ~990, and ~400 Ω/sq, respectively. This indicates that the electrical properties of graphene electrodes are significantly dependent on the types of dopants and the transfer methods. Furthermore, our analysis on pristine graphene sheets formed by the dry-transfer method using field emission scanning electron microscopy (FE-SEM) showed that the graphene sheet had some missing areas (not shown), and therefore, its sheet resistance was much higher than 100−1000 Ω/sq, which is a generally accepted sheet resistance range for graphene. The reason for the missing areas seems to be that some parts of the graphene sheet are being lacerated when it is transferred by silicone/PET films unlike in the case of the conventional wet method. However, the difference in sheet resistances of the two types of graphene reduced markedly with increased layers, and converged to several hundreds of ohms per square at ~12 layers. The reason for the resistance reduction is that the missing areas were gradually filled by additional layers. Eventually, the sheet resistances of the anode (~12 layers) and cathode (~8 layers) used in this study were ~110 and ~741 Ω/sq, respectively, and therefore we could use them as the anode and cathode electrodes for our QD-LEDs.

The variation of transmittance was also measured at a wavelength of 535 nm, corresponding with the peak wavelength of electroluminescence, by using a UV−vis−NIR spectrometer (Lambda 950, PerkinElmer, USA) in order to investigate the optical characteristics of graphene electrodes as a function of the number of layers. Figure 2f illustrates the transmittance data of the graphene electrodes with respect to quartz substrates. We took data five times and averaged them to reduce the measurement uncertainty. Specifically, the figure shows transmittance as a function of the number of layers (1, 2, 4, 8, and 12 layers) and doping (pristine, Au-NP doped, and Ag-NW doped). In general, transmittance (T) of a stacked graphene film is given as $T = (1 + (N\pi\alpha)/2)^{-2} \approx 1 - N\pi\alpha$.[26] Here, T refers to transmittance, α refers to the fine-structure constant, and N refers to the number of graphene layers. Theoretically, the transmittance of graphene is reduced 2.3% per layer.[27] However, these linear fits to the data showed that the transmittance reduction percentages per layer of pristine graphene, Au-NP graphene, and Ag-NW graphene were ~1.34%, ~1.50%, and ~2.44%, respectively. The transmittance reduction rates of the first two samples are lower than theoretically expected value (2.3%), which is likely due to the missing areas generated from the dry transfer process described earlier.

Figure 3 shows UPS spectra around the secondary-electron cutoff of graphene electrodes (anode/cathode) used for the QD-LEDs and of pristine graphene with an equal number of layers (anode, 12 layers; cathode, 8 layers). We obtained the work functions (Φ) of the four samples from the relation, $\Phi = h\nu - E_F - E_{cutoff}$, where

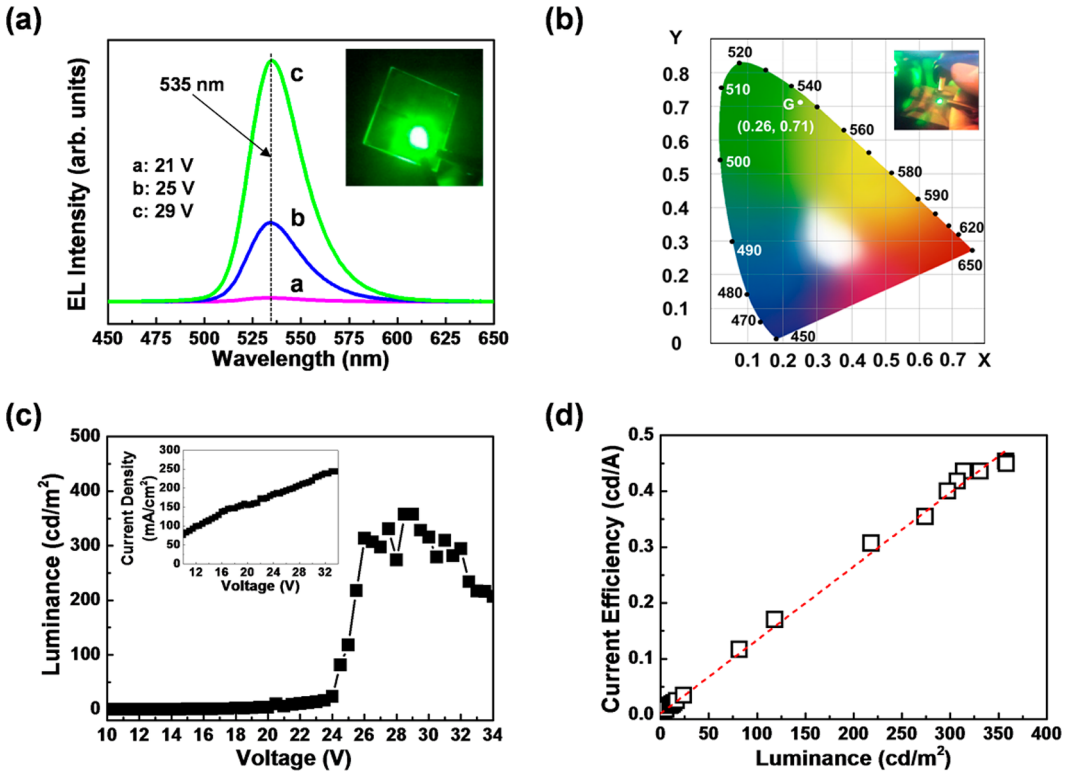

Figure 4. (a) EL spectra of our QD-LED devices with graphene electrodes as a function of applied voltage. The inset shows the green EL image collected at 40 V. (b) The CIE color coordinates corresponding to the green emission spectra in panel a. (c) Voltage-dependent variations of luminance and current density (inset). (d) Current efficiency vs luminance characteristics of our QD-LED.

$h\nu$, E_F, and E_{cutoff} are the energy of the incident photon (21.22 eV), the Fermi level edge, and the secondary-electron cutoff, respectively. Both eight-layered pristine graphene and 12-layered pristine graphene had a similar work function value of ~4.5 eV, which matches the work function previously reported for CVD graphene.[28,29] We note that the 12-layered pristine graphene film shows slightly lower work function than the 8-layered film. In contrast, the work function values of 8-layer Ag-NW doped graphene (blue squares) and 12-layer Au-NP doped graphene (red triangles) were 4.3 eV (decreased by ~0.2 eV) and 4.9 eV (increased by ~0.4 eV), respectively. Accordingly, it was shown that the difference in the work functions of fabricated graphene anodes and cathodes was 0.6 eV.

Voltage-dependent electroluminescent (EL) spectra of the fabricated green QD-LED are shown in Figure 4a. The EL peak wavelength (535 nm) remained unchanged regardless of applied voltage intensity. Compared with organic light-emitting diodes, the present QD-LED exhibited a remarkably narrow full-width at half-maximum (fwhm) of 32 nm, thus affording exceptional color purity.[1,30] The inset of Figure 4a shows an image of green light emitting from the fabricated QD-LED. As designated in Figure 4b, the resulting green EL corresponds to (0.26, 0.71) in the CIE color coordinates. Figure 4c shows a plot of luminance versus voltage up to 34 V. The luminance turn-on voltage was around 20 V, and a maximum luminance for the emissive area was observed as ~358 cd/m^2 at 29 V. Note that all these results are based solely on the light exiting through the quartz substrate. In other words, unlike the case of conventional light-emitting devices, the luminance and current efficiency here do not include light output reflected back from opaque metallic cathodes, owing to the negligible reflectance of Ag-NW graphene cathodes. Additionally, compared with earlier QD-LEDs consisting of ITO anode and Al cathode,[31,32] our device with graphene-based electrodes operates in an appreciably higher voltage range (>20 V), since the turn-on voltage of light-emitting devices is strongly dependent on the sheet resistance of their electrodes.[15] Considering sheet resistances of 10−100 Ω/sq for ITO and <1 Ω/sq for Al, those of our graphene-based electrodes were considerably increased, as shown Figure 2e. The variation of current density as a function of applied voltage showed an unconventionally linear behavior, with a slope of 2.5 mA·cm^{-2}·V^{-1} in the measured voltage range (inset of Figure 4c), which indicates that well-defined ohmic contacts were formed between the graphene sheets and the outermost layers (i.e., HIL and ETL). As shown in Figure 4d, the current efficiency tended to increase with applied voltage, following a similar pattern in Figure 4c. The average maximum current efficiency reached around 0.45 cd/A at 29 V. This value

is much lower than the record value (46.4 cd/A) reported for green QD-LEDs fabricated with conventional electrode materials (i.e., ITO and aluminum).[32] Still, continual improvements of the sheet conductances of graphene electrodes to allow a more efficient charge injection to the QD EML will be required for the fabrication of more efficient and brighter QD-LEDs with graphene electrodes.

CONCLUSIONS

In summary, this study was performed to fabricate a fully transparent QD-LED with the use of graphene-based electrodes. In order to modify pristine graphene with a work function of 4.5 eV for use as anode and cathode electrodes, Au-NP and Ag-NW dopants, respectively, were employed. As a result, the work function values were changed to 4.9 eV (with Au-NP) and 4.3 eV (with Ag-NW), and the Schottky barrier between internal light-emitting layers was nearly zero. In addition, the sheet resistances of 12-layer pristine graphene, Au-NP graphene, and Ag-NW graphene formed by the dry-transfer process using silicone/PET film showed as low as 0.1−0.3% of initial single-layer graphene sheets. The fabricated fully transparent QD-LED with multilayered graphene electrodes showed over 70% transmittance in the visible spectral range. Furthermore, the luminance, current efficiency, and CIE coordinates of the device were ∼358 cd/m^2 at 29 V, ∼0.45 cd/A, and (0.26, 0.71), respectively. Considering the high transparency and flexibility of graphene and plastic-compatible temperatures (≤150 °C) used in every step of fabrication, further optimization of this technique by manipulating sheet resistance and work function and possible combinations with flexible substrates may accelerate the implementation of fully transparent and flexible displays with high efficiency.

EXPERIMENTAL SECTION

Fabrication of Fully Transparent QD-LEDs. A fully transparent QD-LED was fabricated to have a structure consisting of an anode layer (Au-NP graphene with a work function of 4.9 eV), hole injection layer (PEDOT/PSS), hole transfer layer (PVK), emitting layer (CdZnSeS/ZnS QDs), electron transfer layer (ZnO nanoparticles), and cathode layer (Ag-NW graphene with a work function of 4.3 eV). To grow graphene, a piece (∼8 × 3 cm^2) of Cu foil (25 μm thick, Alfa Aesar) was placed in the center of a quartz tube with a diameter of 2 in. After 100 sccm of H_2 gas was flowed into the tube, the native oxide on the surface of the Cu foil was removed by annealing at ∼1000 °C for 1.5 h. Then, under CH_4 gas environment with a flow rate of 20 sccm at the same temperature, annealing was conducted for another 30 min. When it was cooled to room temperature, a single-layer graphene with a uniform thickness was formed on the Cu foil. In order to avoid damaging layers vulnerable to moisture and organic solvents (PEDOT/PSS, PVK, CdZnSeS/ZnS QDs, ZnO nanoparticles), a dry transfer process was employed, where a silicone/polyethylene terephthalate (PET) film was used for the transfer of graphene.[33] The dry transfer process is divided into four steps: (i) placing a piece of graphene/Cu foil between two glass slides and applying consistent pressure to make it as flat as possible; (ii) placing a silicone/PET film to the graphene side of the flattened graphene/Cu foil; (iii) leveling the graphene/silicone/PET film between the two glass slides by applying pressure; (iv) facing the bare Cu side area downward and putting it in a copper etchant (CE-100, Transene Company) solution (20 min) and rinsing the graphene with silicone/PET film in deionized water several times to remove the etchant residue completely. As a final step in producing the graphene electrodes, the fabricated graphene/silicone/PET was put on the surface of a quartz substrate (for anodes) or on the top of a ZnO nanoparticle-layer (for cathodes), and then only the silicone/PET film was carefully peeled off.

To manipulate the work function of the graphene to be used as anodes and cathodes, two different types of dopants were used.[34] For the graphene anode, $AuCl_3$ solution (5 mM) was spin-cast on a graphene layer at 1000 rpm for 30 s. Here, 150 °C hot-plate annealing was conducted after the spin-casting of $AuCl_3$ solution, and a $Au^{3+} \rightarrow Au^0$ reaction occurred on the graphene surface, achieving a graphene electrode with p-type characteristics.[34,35] The total thickness of the graphene anode was the sum of 12 layers of graphene and the Au-nanoparticles (NPs) inserted alternately.

On top of the anode, 20 nm-thick poly(ethylenedioxythiophene)/polystyrenesulfonate (PEDOT/PSS) as a hole injection layer (HIL) was spin-cast at 3000 rpm for 60 s. On top of the HIL, a 20 nm-thick hole transport layer (HTL) was generated by spin-depositing a solution of 0.05 g of PVK (average M_W = 25000−50000) dissolved in 5 mL of chlorobenzene. Then, CdZnSeS/ZnS QD hexane dispersion with an optical density of ∼3.0 at an excitonic absorption peak was spin-cast at 2000 rpm for 20 s, forming a ∼45 nm-thick QD emitting layer (EML). A 40 nm-thick electron transport layer (ETL) was then formed by spin-depositing a ZnO nanoparticle−ethanol dispersion with a concentration of 25−30 mg/mL. The above constituent layers were baked for 30 min individually after each spin-deposition at 150, 150, 60, and 60 °C for HIL, HTL, EML, and ETL, respectively.

Meanwhile, the deposition process for the graphene-based cathode electrode is as follows: transferring a graphene sheet that was not doped was performed using a silicone/PET film at first; repetitively stacking graphene sheets doped with Ag-nanowires (NWs) up to eight layers. The Ag-NW doping was carried out by facing the graphene side of the graphene/silicone/PET combination layer upward to perform spin-casting directly on the surface of graphene (1500 rpm, 60 s), since isopropyl alcohol (IPA) comprising the Ag-NW solvent might induce a lytic reaction if it is contacted with the aforementioned multilayer (with ZnO nanoparticles exposed). The resulting Ag-NW graphene/silicone/PET stack was evenly placed to the target surface and then the silicone/PET film was peeled off carefully from the surface underneath. In the same manner, Ag-NW graphene was repetitively stacked. Finally, an additional annealing process was performed in vacuum, at about 2 × 10^{-6} Torr and below 150 °C, to enhance the contact resistance between graphene electrodes and the active layers in the fabricated QD-LED.

Materials and Device Characterization. Raman spectra were taken with a confocal and micro-Raman system (ACRON, UniNanotech, Korea). The excitation source was a 532 nm laser (2.33 eV). Sheet resistance data were taken using a four-point probe measurement (CMT-SR1000N, Chang Min Co., LTD, Korea). Transmittance spectra were measured by using a UV−vis−NIR spectrometer (Lambda 950, PerkinElmer, USA) in the range of 200−2000 nm wavelength. Ultraviolet photoemission spectroscopy (UPS) was performed using a Kratos Analytical AXIS-Nova spectrometer with a He I discharge lamp ($h\nu$ = 21.22 eV). EL spectra and luminance−current density−voltage characteristics of the QD-LEDs were recorded with a Konica-Minolta CS-1000 spectroradiometer coupled with a Keithley 2400 voltage and current source under ambient conditions.

Conflict of Interest: The authors declare no competing financial interest.

Acknowledgment. This research was supported by the National Research Foundation of Korea (Nos. 2012R1A2A2A01013734, 2012R1A1A2041150, and 2013R1A2A2A01068158) through the Ministry of Science, ICT and Future Planning, and MSIP, Korea.

REFERENCES AND NOTES

1. Sun, Q.; Wang, Y. A.; Li, L. S.; Wang, D.; Zhu, T.; Xu, J.; Yang, C.; Li, Y. Bright, Multicoloured Light-Emitting Diodes Based on Quantum Dots. *Nature* **2007**, *1*, 717–722.
2. Kwak, J.; Bae, W. K. Bright and Efficient Full-Color Colloidal Quantum Dot Light-Emitting Diodes Using an Inverted Device Structure. *Nano Lett.* **2012**, *12*, 2362–2366.
3. Li, J.; Hu, L.; Wang, L.; Zhou, Y.; Grüner, G.; Marks, T. J. Organic Light-Emitting Diodes Having Carbon Nanotube Anodes. *Nano Lett.* **2006**, *6*, 2472–2477.
4. Xu, F.; Zhu, W. Q.; Yan, L.; Xu, H.; Xiong, L. H.; Li, J. H. Single Walled Carbon Nanotube Anodes Based High Performance Organic Light-Emitting Diodes with Enhanced Contrast Ratio. *Org. Electron.* **2012**, *13*, 302–308.
5. Zhang, D.; Wang, R.; Wen, M.; Weng, D.; Cui, X.; Sun, J.; Li, H.; Lu, Y. Synthesis of Ultralong Copper Nanowires for High-Performance Transparent Electrodes. *J. Am. Chem. Soc.* **2012**, *134*, 14283–14286.
6. Kholmanov, I. N.; Magnuson, C. W.; Aliev, A. E.; Li, H.; Zhang, B.; Suk, J. W.; Zhang, L. L.; Peng, E.; Mousavi, S. H.; Khanikaev, A. B.; et al. Improved Electrical Conductivity of Graphene Films Integrated with Metal Nanowires. *Nano Lett.* **2012**, *12*, 5679–5683.
7. Kim, A.; Won, Y.; Woo, K.; Kim, C.-H.; Moon, J. Highly Transparent Low Resistance ZnO/Ag Nanowire/ZnO Composite Electrode for Thin Film Solar Cells. *ACS Nano* **2013**, *7*, 1081–1092.
8. Wu, J.; Agrawal, M.; Becerril, H. A.; Bao, Z.; Liu, Z.; Chen, Y.; Peumans, P. Organic Light-Emitting Diodes on Solution-Processed Graphene Transparent Electrodes. *ACS Nano* **2010**, *4*, 43–48.
9. Zhu, X.-Z.; Han, Y.-Y.; Liu, Y.; Ruan, K.-Q.; Xu, M.-F.; Wang, Z.-K.; Jie, J.-S.; Liao, L.-S. The Application of Single-Layer Graphene Modified with Solution-Processed TiO_x and PEDOT:PSS as a Transparent Conductive Anode in Organic Light-Emitting Diodes. *Org. Electron.* **2013**, *14*, 3348–3354.
10. Kim, K. S.; Zhao, Y.; Jang, H.; Lee, S. Y.; Kim, J. M.; Kim, K. S.; Ahn, J.-H.; Kim, P.; Choi, J.-Y.; Hong, B. H. Large-Scale Pattern Growth of Graphene Films for Stretchable Transparent Electrodes. *Nature* **2009**, *457*, 706–710.
11. Kwon, K. C.; Choi, K. S.; Kim, B. J.; Lee, J.-L.; Kim, S. Y. Work-Function Decrease of Graphene Sheet Using Alkali Metal Carbonates. *J. Phys. Chem. C* **2012**, *116*, 26586–26591.
12. Shin, H.-J.; Choi, W. M.; Choi, D.; Han, G. H.; Yoon, S.-M.; Park, H.-K.; Kim, S.-W.; Jin, Y. W.; Lee, S. Y.; Kim, J. M.; et al. Control of Electronic Structure of Graphene by Various Dopants and Their Effects on a Nanogenerator. *J. Am. Chem. Soc.* **2010**, *132*, 15603–15609.
13. Meina, H.; Lin, Y.-C.; Obergfell, D.; Chiu, P.-W. Tuning of Charge Densities in Graphene by Molecule Doping. *Adv. Funct. Mater.* **2011**, *21*, 2687–2692.
14. Kwon, K. C.; Choi, K. S.; Kim, S. Y. Increased Work Function in Few-Layer Graphene Sheets via Metal Chloride Doping. *Adv. Funct. Mater.* **2012**, *22*, 4724–4731.
15. Han, T.-H.; Lee, Y.; Choi, M.-R.; Woo, S.-H.; Bae, S.-H.; Hong, B. H.; Ahn, J.- H.; Lee, T.-W. Extremely Efficient Flexible Organic Light-Emitting Diodes with Modified Graphene Anode. *Nat. Photonics* **2012**, *6*, 105–110.
16. Chandramohan, S.; Kang, J. H.; Katharria, Y. S.; Han, N.; Beak, Y. S.; Ko, K. B.; Park, J. B.; Kim, H. K.; Suh, E.-K.; Hong, C.-H. Work-Function-Tuned Multilayer Graphene as Current Spreading Electrode in Blue Light-Emitting Diodes. *Appl. Phys. Lett.* **2012**, *100*, No. 023502.
17. Chung, K.; Lee, C.-H.; Yi, G.-C. Transferable GaN Layers Grown on ZnO-Coated Graphene Layers for Optoelectronic Devices. *Science* **2010**, *330*, 655–657.
18. Sun, T.; Wang, Z. L.; Shi, Z. J.; Ran, G. Z.; Xu, W. J.; Wang, Z. Y.; Li, Y. Z.; Dai, L.; Qin, G. G. Multilayered Graphene Used as Anode of Organic Light Emitting Devices. *Appl. Phys. Lett.* **2010**, *96*, No. 133301.
19. Kim, S.-Y; Kim, J.-J. Outcoupling Efficiency of Organic Light Emitting Diodes Employing Graphene as the Anode. *Org. Electron.* **2012**, *13*, 1081–1085.
20. Han, Y.; Zhang, L.; Zhang, X.; Ruan, K.; Cui, L.; Wang, Y.; Liao, L.; Wang, Z.; Jie, J. Clean Surface Transfer of Graphene Films via an Effective Sandwich Method for Organic Light-Emitting Diode Applications. *J. Mater. Chem. C* **2014**, *2*, 201–207.
21. Bae, S.; Kim, H.; Lee, Y.; Xu, X.; Park, J.-S.; Zheng, Y.; Balakrishnan, J.; Lei, T.; Kim, H. R.; Song, Y. I.; et al. Roll-to-Roll Production of 30-Inch Graphene Films for Transparent Electrodes. *Nat. Nanotechnol.* **2010**, *5*, 574–578.
22. Wang, Y. Y.; Ni, Z. H.; Shen, Z. X.; Wang, H. M.; Wu, Y. H. Interference Enhancement of Raman Signal of Graphene. *Appl. Phys. Lett.* **2008**, *92*, No. 043121.
23. Das, A.; Pisana, S.; Chakraborty, B.; Piscanec, S.; Saha, S. K.; Waghmare, U. V.; Novoselov, K. S.; Krishnamurthy, H. R.; Geim, A. K.; Ferrari, A. C.; et al. Monitoring Dopants by Raman Scattering in an Electrochemically Top-Gated Graphene Transistor. *Nat. Nanotechnol.* **2008**, *3*, 210–215.
24. Ryu, S.; Liu, L.; Berciaud, S.; Yu, Y.-J.; Liu, H.; Kim, P.; Flynn, G. W.; Brus, L. E. Atmospheric Oxygen Binding and Hole Doping in Deformed Graphene on a SiO_2 Substrate. *Nano Lett.* **2010**, *10*, 4944–4951.
25. Ni, Z. H.; Wang, H. M.; Luo, Z. Q.; Wang, Y. Y.; Yu, T.; Wu, Y. H.; Shen, Z. X. The Effect of Vacuum Annealing on Graphene. *J. Raman Spectrosc.* **2010**, *41*, 479–483.
26. Kuzmenko, A. B.; Heumen, E.; Carbone, F.; Marel, D. Universal Optical Conductance of Graphite. *Phys. Rev. Lett.* **2008**, *100*, No. 117401.
27. Nair, R. R.; Blake, P.; Grigorenko, A. N.; Novoselov, K. S.; Booth, T. J.; Stauber, T.; Peres, N. M. R.; Geim, A. K. Fine Structure Constant Defines Visual Transparency of Graphene. *Science* **2008**, *320*, 1308.
28. Kim, D.; Lee, D.; Lee, Y.; Jeon, D. Y. Work-Function Engineering of Graphene Anode by Bis(trifluoromethanesulfonyl)-amide Doping for Efficient Polymer Light-Emitting Diodes. *Adv. Funct. Mater.* **2013**, *23*, 5049–5055.
29. Lin, W.-H.; Chen, T.-H.; Chang, J.-K.; Taur, J.-I.; Lo, Y.-Y.; Lee, W.-L; Chang, C.-S.; Su, W.-B.; Wu, C.-I. A Direct and Polymer-Free Method for Transferring Graphene Grown by Chemical Vapor Deposition to Any Substrate. *ACS Nano* **2014**, *8*, 1784–1791.
30. Caruge, J. M.; Halpert, J. E.; Wood, V.; Bulovic, V.; Bawendi, M. G. Colloidal Quantum-Dot Light-Emitting Diodes With Metal-Oxide Charge Transport Layers. *Nat. Photonics* **2008**, *2*, 247–250.
31. Lee, K.-H.; Lee, J.-H.; Song, W.-S.; Ko, H.; Lee, C.; Lee, J.-H.; Yang, H. Highly Efficient, Color-Pure, Color-Stable Blue Quantum Dot Light-Emitting Devices. *ACS Nano* **2013**, *7*, 7295–7302.
32. Lee, K.-H.; Lee, J.-H.; Kang, H.-D.; Park, B.; Kwon, Y.; Ko, H.; Lee, C.; Lee, J.; Yang, H. Over 40 cd/A Efficient Green Quantum Dot Electroluminescent Device Comprising Uniquely Large-Sized Quantum Dots. *ACS Nano* **2014**, *8*, 4893–4901.
33. Chen, X.-D.; Liu, Z.-B.; Zheng, C. -Y; Xing, F.; Yan, X.-Q.; Chen, Y.; Tian, J.-G. High-Quality and Efficient Transfer of Large-Area Graphene Films onto Different Substrates. *Carbon* **2013**, *56*, 271–278.
34. Shi, Y.; Kim, K. K.; Reina, A.; Hofmann, M.; Li, L.-J.; Kong, J. Work Function Engineering of Graphene Electrode via Chemical Doping. *ACS Nano* **2010**, *4*, 2689–2694.
35. Günes, F.; Shin, H.-J.; Biswas, C.; Han, G. H.; Kim, E. S.; Chae, S. J.; Choi, J.-Y.; Lee, Y. H. Layer-by-Layer Doping of Few-Layer Graphene Film. *ACS Nano* **2010**, *4*, 4595–4600.